NaGdS2: A Promising Sulfide for Cryogenic Magnetic Cooling

Charlène Delacotte, Tatiana Pomelova, Thomas Stephant, Thierry Guizouarn, Stéphane Cordier, Nikolay Naumov, Pierric Lemoine

$NaGdS_2$: a promising sulfide for cryogenic magnetic cooling

Charlène Delacotte,[a] Tatiana A. Pomelova,[b] Thomas Stephant,[a] Thierry Guizouarn,[a] Stéphane Cordier,[a] Nikolay G. Naumov,[b] Pierric Lemoine,[a,*]

[a] Univ Rennes, CNRS, Institut des Sciences Chimiques de Rennes – UMR 6226, F-35000 Rennes, France

[b] Nikolaev Institute of Inorganic Chemistry SB RAS, 3, Akad. Lavrentiev Ave., 630090 Novosibirsk, Russian Federation

* pierric.lemoine@univ-rennes1.fr

KEYWORDS sulfide, powder X-ray diffraction, crystal chemistry, magnetic material, magnetic refrigeration.

ABSTRACT: The development of effective and eco-friendly cooling technology demands an investigation of new magnetocaloric materials. Compounds containing gadolinium are one of the best candidates due to the large spin-only magnetic moment of Gd^{3+} ion. This work reports on the magnetocaloric properties of the $AGdS_2$ family (A = Li, Na, K, Rb) in relation to crystal chemistry of these compounds. These sulfides crystallize in two different structure-types: NaCl (A = Li) and α-$NaFeO_2$ (A = Na, K, Rb). Although one would expect the larger magnetocaloric effect to be associated to $LiGdS_2$ due to its higher magnetic/non-magnetic mass ratio, our study demonstrates that the $NaGdS_2$ member leads to the best properties among the investigated series. The change of structure from the 3D NaCl structure of $LiGdS_2$ to the layered α-$NaFeO_2$ structure of $NaGdS_2$ drastically improves the magnetocaloric properties. Hence, thanks to its structural features associated to negligible exchange interactions, $NaGdS_2$ exhibits a magnetic entropy change up to 54 J kg^{-1} K^{-1} at 2.5 K for $\mu_0\Delta H$ = 5 T, which is comparable to the top ranked inorganic Gd-based materials operating in the cryogenic temperature range. These magnetocaloric figures of merit provide evidence that Gd-based sulfides are promising materials for magnetic refrigeration and, more broadly, this highlights the potential of sulfides in that field.

INTRODUCTION

There is currently an intense research activity for designing magnetocaloric materials for potential magnetic refrigeration either near room temperature for refrigeration and air conditioning, or at cryogenic temperature for gas liquefaction or ultra-low temperature applications.[1-10] Magnetic refrigeration, based on the magnetocaloric effect,[2] is a known alternative to the scarce helium-3 for sub-Kelvin cooling applications.[11] Compared with vapor to liquid cooling technologies, this solid-state alternative has higher cooling performance via adiabatic demagnetization cooling, as first demonstrated with the paramagnetic salt $Gd_2(SO_4)_3{\cdot}8H_2O$.[12]

The large spin-only magnetic moment of Gd^{3+} ion (S = 7/2) promotes a large magnetic entropy change with negligible magnetic hysteresis. Moreover, gadolinium compounds are usually characterized by low temperature magnetic ordering and by weak exchange interactions that give rise to a large magnetic entropy change. This makes Gd-based materials the most popular magnetocaloric refrigerants for cryogenic applications. The following materials are cited examples of promising Gd-based magnetocalorics: inorganic paramagnetic salts such as $Gd_2(SO_4)_3{\cdot}8H_2O$,[12] oxides such as $Gd_3Ga_5O_{12}$,[13-15] Gd_2FeCoO_6,[16] $GdCrO_4$,[17-18] and $GdVO_4$,[19] intermetallics such as $GdPd_2Si$,[20-24] borides, carbides and borocarbides such as $GdCo_2B_2$,[25-28] and many molecular organometallic materials, including metal and cluster complexes, metal-organic frameworks and polymers.[7,29-38] Note that for room-temperature refrigeration, while $Gd_5Si_2Ge_2$ is still a reference material,[39] Mn-based compounds have become best candidates as they are free of "critical" elements.[40-43]

Considering that the increase of refrigerant efficiency near liquid helium temperature requires materials with weak exchange interactions,[44-45] as well as large magnetic/non-magnetic mass and volume ratio, recent studies focused on inorganic Gd-based complexes with light and small ligands such as PO_4^{3-}, BO_3^{3-}, SO_4^{2-}, CO_3^{2-}, HCO_2^-, BH_4^-, HO^-, or F^-. This leads to inorganic materials with huge magnetocaloric effect near liquid helium temperature,[46-56] such as $GdPO_4$,[46] $K_3Li_3Gd_7(BO_3)_9$,[47] $GdBO_3$,[48] $Gd_2Cu(SO_4)_2(OH)_4$,[49] $Gd(OH)SO_4$,[50] $Gd(OH)CO_3$,[51] $Gd(HCO_2)_3$,[52-53] $Gd(BH_4)_3$,[54] $K_2Gd(BH_4)_5$,[54] $Cs_3Gd(BH_4)_6$,[54] $Gd(OH)_3$,[55] $Gd_2O(OH)_4(H_2O)_2$,[55] and GdF_3.[56]

Surprisingly, only few articles focused on the magnetocaloric properties of inorganic sulfides and oxysulfides.[57-63] EuS is characterized by a significant magnetocaloric effect at T_C = 16.5 K, with a maximum magnetic entropy change from bulk of 16.8 J kg^{-1} K^{-1} and 28.4 J kg^{-1} K^{-1} for magnetic field changes of 2 T and 5 T, respectively.[58] Orthorhombic α-Ln_2S_3 (Ln = Tb, Dy) compounds are characterized by two successive antiferromagnetic transitions (T_N < 15 K), which can be shifted to either lower or higher temperature (depending of the crystal orientation) by a magnetic field change, reflecting a strong magnetic anisotropy of the materials.[62] Consequently, their magnetocaloric effect is reported to be controllable by changing the magnitude and orientation of the magnetic field. $FeCr_2S_4$, $CoCr_2S_4$ and $CdCr_2S_4$ compounds are characterized by a second order magnetic transition at 166 K, 225 K and 87 K,[59,60,63] leading to significant magnetic entropy changes of 3.72 J kg^{-1} K^{-1} ($\mu_0\Delta H$ = 5T), 3.99 J kg^{-1} K^{-1} ($\mu_0\Delta H$ = 5T)[63] and 3.95 J kg^{-1} K^{-1} ($\mu_0\Delta H$ = 2T),[60] respectively. Zheng et al. showed that the magnetic transition of $CoCr_2S_4$ can be shifted to higher temperature by Cu for Co substitution, allowing to reach a $-\Delta S_M$ value of 2.57 J kg^{-1} K^{-1} for $\mu_0\Delta H$ = 5T at room temperature for the $Co_{0.4}Cu_{0.6}Cr_2S_4$ compound.[59] These studies demonstrate the potential of inorganic sulfides as magnetic refrigerants either near room temperature with transition metals as magnetic elements or at low temperature with lanthanides as magnetic centers.

However, for potential applications near liquid helium temperature, it appears necessary to find sulfide materials having weaker magnetic interactions.

$ALnS_2$ alkali lanthanide sulfides have been previously investigated from the structural point of view,[64-69] but only few reports are available about their physical properties.[66,67,70] In this study, we focus on the Gd-based sulfide series, i.e. the $AGdS_2$ compounds with A = Li, Na, K, and Rb. Their magnetic and magnetocaloric properties are assessed and discussed in relation with their structural features. To support our discussion, a comparison with structures and properties of some binary and ternary Gd-based sulfides, oxide and oxysulfide is addressed. While the design of phases with large magnetic/non-magnetic mass and volume ratio will allow to make more competitive materials for potential refrigerant applications, the magnetocaloric effect reported for the $NaGdS_2$ member reminds that crystal structure still governs the magnetic exchange interactions and open the route to consider Gd-based sulfides as new promising magnetorefrigerants near liquid helium temperature.

EXPERIMENTAL SECTION

Synthesis. $AGdS_2$ (A = Li-Rb) phases were prepared starting from A_2CO_3 (A = Li-Rb) and Gd_2S_3 with the 30:1 molar ratio (note that Gd_2S_3 was prepared by the chemical reaction of high-purity Gd_2O_3 as described by Ohta et al.[71]). The mixture was loaded into glassy carbon boat and placed in a quartz reactor. A flow of Ar with products of NH_4SCN thermal decomposition (mainly, H_2S+CS_2) were applied through the reactor and temperature was slowly raised to 700-1000°C. After annealing for 2 hours, the reactor was cooled to room temperature, and the resulting product washed by water and dried by ethanol. Note that the sulfidizing gas mixture contains highly toxic CS_2, H_2S and NH_3. This procedure controlled risk by bubbling the gaseous sulfidation products through $ZnSO_4$ solution. All operations should be held in a fume hood.

$CsGdS_2$ was prepared starting from Gd_2S_3 and Cs_2S_x. First, mixture of cesium polysulfides Cs_2S_x (mainly, Cs_2S_6) was prepared at 300°C from Cs_2CO_3.[72] Then S, Gd_2S_3 and Cs_2S_x (15:1: ~2.5 molar ratio) were loaded in glassy carbon boat and placed in a quartz reactor. The mixture was heated to 1000°C under Ar flow, maintained at this temperature during 30 min and cooled to room temperature. The resulting product was rapidly washed by water and dried by ethanol, and thoroughly ground afterwards.

Sulfides $Gd_{10}S_{19}$ and Gd_2S_3, and oxysulfide Gd_2O_2S were synthesized using Gd (99.9 at.%, Alfa Aesar), S (99.9 at.%, Strem Chemicals) and Gd_2O_3 (99.99 at.%, Alfa Aesar) commercial powders as starting materials. For each compound, powders were weighed in stoichiometric ratios and ground together in an agate mortar. The mixture was then put into a silica tube and sealed under vacuum ($\approx 10^{-2}$ mbar). The ampule was finally placed in a tubular furnace and heated for 96h at 500°C (Gd_2S_3) or 750°C ($Gd_{10}S_{19}$ and Gd_2O_2S).

These synthesis protocols allowed us to prepare high quality $AGdS_2$ (A = Li, Na, K, Rb), $Gd_{10}S_{19}$, Gd_2S_3 and Gd_2O_2S powder samples with purity suitable for magnetocaloric characterizations. Only a small amount of Gd_2O_2S oxysulfide was detected by powder X-ray diffraction analysis in the $AGdS_2$ (A = Na, K, Rb) samples, as well as, minor extra peaks corresponding to an unknown phase in the $RbGdS_2$ sample.

Powder X-ray diffraction. Powder X-ray diffraction analyses were carried out to determine the sample purity and crystal structure of the constituting phases (Figures S1-S7) using a Bruker D8 advance diffractometer equipped with a Cu X-ray tube (Kα1), a Ge [111] monochromator, and a LynxEye detector. Refinements of the powder X-ray diffraction patterns were performed using the Fullprof software included in the WinPlotr package.[73-74]

Magnetic measurements. Magnetic and magnetocaloric measurements were performed on polycrystalline samples using a SQUID magnetometer (MPMS XL5, Quantum Design). Zero field cooled (ZFC) measurement was carried out from 1.8 to 300 K at a constant applied magnetic field of 0.1 T. The magnetocaloric properties were determined from magnetic entropy change, $-\Delta S_M$, evaluated using one of the Maxwell relations:

$$\Delta S_M(T)_{\Delta H} = \int_0^{H_f} \left(\frac{\partial M(T,H)}{\partial T}\right)_H dH \quad (1)$$

The numerical integration of Eq. (1) was carried out using the method proposed by Pecharsky and Gschneidner Jr.,[75] from magnetization isotherms recorded on heating from 2 K to 20 K in applied magnetic fields up to 5 T, with field steps of 0.2 T and temperature increments of 1 K.

RESULTS AND DISCUSSION

Structural features. According to powder X-ray diffraction data, the $AGdS_2$ (A = Li, Na, K, Rb) sulfides are characterized by either the cubic NaCl structure type or the rhombohedral α-$NaFeO_2$ structure type. $LiGdS_2$ forms with the NaCl cubic structure (Figure S1) while other members crystallize with the rhombohedral α-$NaFeO_2$ structure (Figures S2-S4). Crystallographic parameters refined from powder X-ray diffraction data recorded at room temperature are given in Table 1 and the corresponding structural models are shown in Figure 1.

Table 1. Refined crystallographic data of the $AGdS_2$ (A = Li, Na, K, Rb) compounds.

Compound	$LiGdS_2$	$NaGdS_2$	$KGdS_2$	$RbGdS_2$
Structure type	NaCl	α-$NaFeO_2$		
Crystal system	Cubic	trigonal		
Space group	$Fm\bar{3}m$	$R\bar{3}m$		
a (Å)	5.5299(1)	4.0134(1)	4.0771(1)	4.1172(1)
c (Å)	--	19.9187(4)	21.9170(8)	24.0408(5)
V (Å^3)	169.10(1)	277.86(1)	315.51(2)	352.93(1)
Z	2	3	3	3

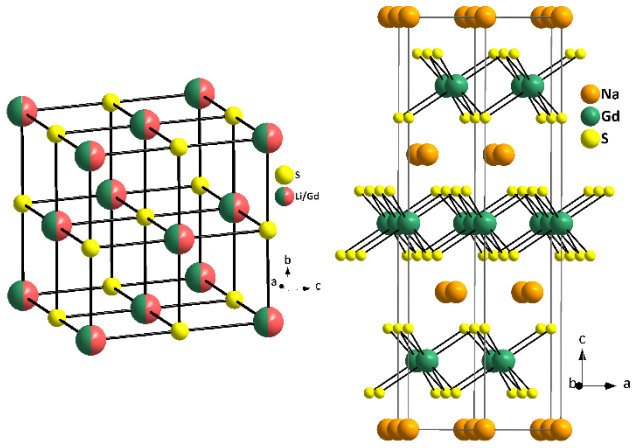

Figure 1. Representation of the crystal structures encountered in the $AGdS_2$ family: (left) NaCl-type with A = Li and (right) α-$NaFeO_2$-type with A = Na, K and Rb.

Magnetic and magnetocaloric properties. In order to shed light on the structure-properties relationships of the $AGdS_2$ (A = Li, Na, K, Rb) series, magnetic and magnetocaloric properties will be presented by drawing a parallel between $LiGdS_2$ (NaCl structure type) and $NaGdS_2$ (α-$NaFeO_2$ structure type) compounds. For the other members, the results are shown in Supporting Information (Figures S8-S10).

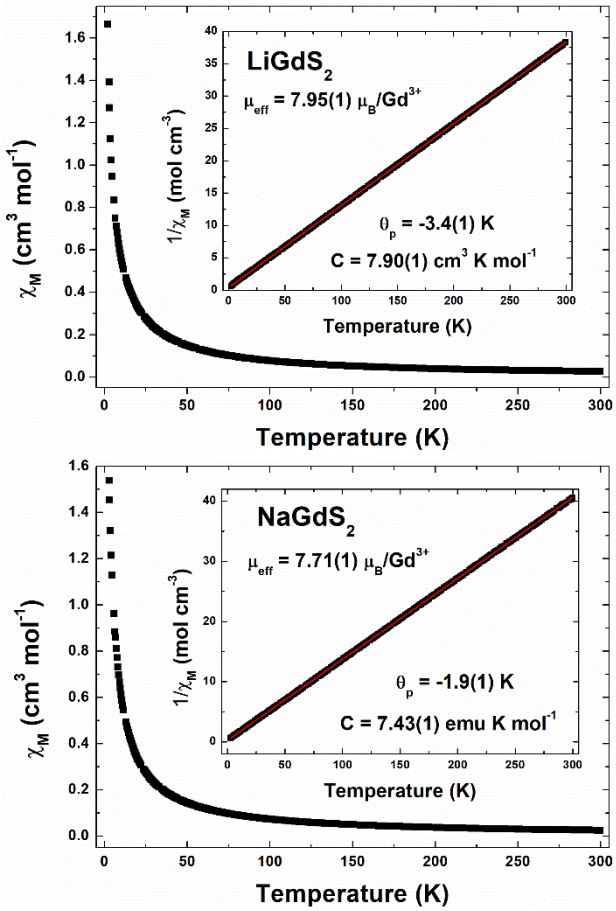

Figure 2. Temperature dependence of the molar magnetic susceptibility (χ_M) of (top) $LiGdS_2$ and (bottom) $NaGdS_2$ recorded from 1.8 K to 300 K under an applied magnetic field of 0.1 T. Corresponding inverse of magnetic susceptibility ($1/\chi_M$) curves fitted from 1.8 K to 300 K with the Curie-Weiss law are shown in insets.

For the whole $AGdS_2$ family, the magnetic susceptibility curves do not indicate a magnetic phase transition within the investigated temperature range (1.8K-300K) as illustrated on Figures 2 and S8. This indicates that all members of the family are paramagnets. The inverse of magnetic susceptibility data were analyzed using the Curie-Weiss law $\chi_M=C/(T-\theta_p)$ where χ_M is the magnetic susceptibility, C is the Curie constant, T is the absolute temperature and θ_p is the paramagnetic Curie-Weiss temperature. All compounds obey to the Curie-Weiss law over the entire temperature range as shown in insets of Figures 2 and S8. Outcomes of the inverse of magnetic susceptibility fits are summarized in Table 2. Resulting effective magnetic moment μ_{eff}/Gd^{3+} values agree with the theoretical one expected for Gd^{3+} free ion (i.e. 7.94 μ_B). The Curie-Weiss fitting parameters indicate small and negative paramagnetic temperatures θ_P for the whole series (ranging from -1.9 K for $NaGdS_2$ to -3.7 K for $KGdS_2$) suggesting the existence of very weak local antiferromagnetic interactions whatever the crystal structure.

From magnetic susceptibility curves, $LiGdS_2$ and $NaGdS_2$ exhibit similar profiles, but in contrast, magnetization data recorded at 2 K evidence two distinct behaviors (Figure 3). Near and below liquid helium temperature, the $NaGdS_2$ magnetization curves tend to follow a Brillouin function, while those of the $LiGdS_2$ compound are still almost linearly field dependent leading to a magnetization far from saturation even under an applied magnetic field of 5 T. This latter feature indicates the existence of local magnetic frustrations suggesting a spin glass behavior for $LiGdS_2$. Moreover, this means that the nature and the strength of the local magnetic coupling characterizing $LiGdS_2$ and $NaGdS_2$ are likely to be different and influenced by the crystal structure.

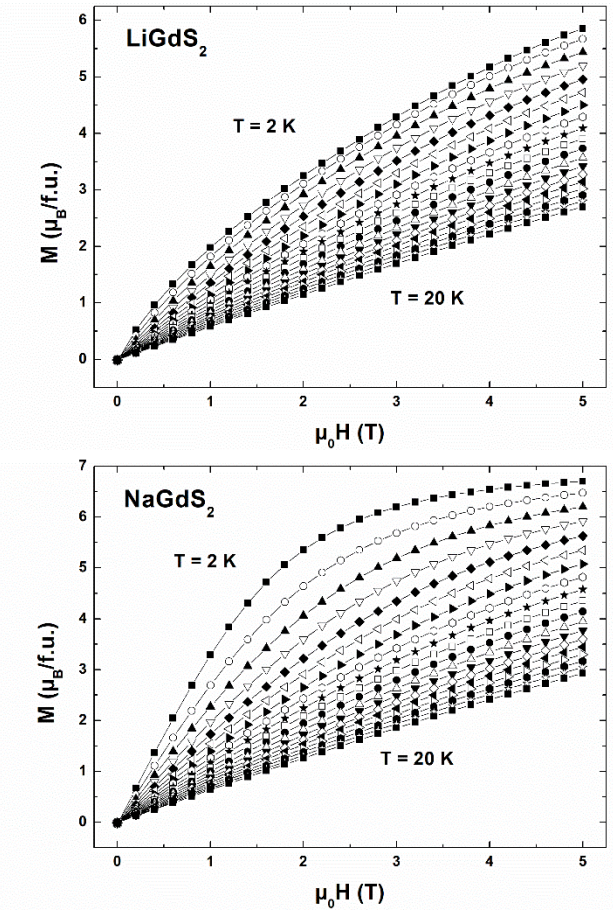

Figure 3. Magnetization isotherms of (top) $LiGdS_2$ and (bottom) $NaGdS_2$ recorded from 2 K to 20 K in applied magnetic fields up to 5 T, with field steps of 0.2 T and temperature increments of 1 K.

The absence of magnetic ordering down to 1.8 K and the very weak local magnetic interactions constitute encouraging experimental features for an interesting magnetocaloric effect near liquid helium temperature. These two points added to (i) the large spin-only magnetic moment of Gd^{3+} ion (S = 7/2) favoring a large magnetic entropy change with negligible magnetic hysteresis and (ii) the high magnetic/non-magnetic mass ratio of the $AGdS_2$ family, led us to investigate their magnetocaloric properties. The magnetic entropy change was then determined for the whole series from isothermal magnetization curves recorded on heating from 2 K to 20 K in applied magnetic fields up to 5 T (Figures 3 and S9).

Table 2. Magnetic properties (fitted effective magnetic moments μ_{eff} and paramagnetic Curie-Weiss temperatures θ_P) and magnetocaloric properties (mass and volume magnetic entropy change) of the $AGdS_2$ series (A = Li, Na, K, Rb).

		Magnetic properties		Magnetocaloric properties					
Compound	Structure type	μ_{eff} (μ_B/Gd^{3+})	θ_P (K)	T (K)	$-\Delta S_M^{max}$ (J kg^{-1} K^{-1})		$-\Delta S_M^{max}$ (mJ cm^{-3} K^{-1})		ρ_{calc} (g cm^{-3})
					0-2 T	0-5 T	0-2 T	0-5 T	
$LiGdS_2$	NaCl	7.95(1)	-3.4(1)	4.5	6.8	23.3	30.2	104.2	4.48
$NaGdS_2$	α-$NaFeO_2$	7.71(1)	-1.9(1)	2.5	23.5	54.0	102.8	236.7	4.38
$KGdS_2$	α-$NaFeO_2$	7.32(1)	-3.7(1)	2.5	14.6	43.6	60.3	179.5	4.11
$RbGdS_2$	α-$NaFeO_2$	7.23(1)	-3.3(1)	2.5	10.0	32.6	46.1	149.9	4.60

For each $AGdS_2$ member, the highest values of mass and volume magnetic entropy change $-\Delta S_M^{max}$ are reported in Table 2 for an applied magnetic field variation of 2 T and 5 T. The best magnetocaloric effect, with values reaching 54 J kg^{-1} K^{-1} (or 236.7 mJ cm^{-3} K^{-1}) at 2.5 K for $\mu_0\Delta H$ = 5 T, is obtained for the $NaGdS_2$ compound while $LiGdS_2$ exhibits moderate magnetocaloric properties at low temperature (23.3 J kg^{-1} K^{-1} (or 104.2 mJ cm^{-3} K^{-1}) at 4.5 K for $\mu_0\Delta H$ = 5 T). As it was suspected from the magnetization data profiles at low temperature (Figure 3), the two structure types induce different local magnetic interactions and consequently sharply affect the magnetocaloric properties. This is illustrated by the effect intensity of $LiGdS_2$ which is about 2 times weaker than that of $NaGdS_2$. Moreover, even when the magnetic/non-magnetic mass ratio decreases (i.e. for A = K and Rb), the magnetocaloric effect of the α-$NaFeO_2$ structure type materials is still higher than that of the NaCl structure type compound.

Figure 4 shows the evolution of the mass magnetic entropy change versus temperature for the two prototypical compounds of the $AGdS_2$ family. The magnetocaloric effect of $NaGdS_2$ continuously increases upon cooling (as well as that of $KGdS_2$ and $RbGdS_2$, Figure S10) while $LiGdS_2$ reaches a maximum at 4.5 K for $\mu_0\Delta H$ = 5 T. This maximum decreases to lower temperatures for lower magnetic field variations. The decrease of the magnetic entropy change of $LiGdS_2$ at very low temperature can be related to the existence of local magnetic frustrations, likely leading to a spin glass behavior, as already discussed from its magnetic susceptibility data. Once again, this is an evidence of the impact of the crystal structure on the magnetocaloric properties of the $AGdS_2$ series.

Discussion. This study shows that the two different crystal structures (i.e. NaCl and α-$NaFeO_2$) encountered in the $AGdS_2$ (A = Li, Na, K, Rb) family strongly affect their physical properties. Based on magnetic measurements, and in particular on the magnetization curve profiles at 2 K, one can observe that the NaCl structure type of $LiGdS_2$ is associated to stronger magnetic couplings compared to the α-$NaFeO_2$ structure type of $NaGdS_2$, $KGdS_2$ or $RbGdS_2$. The strength of the magnetic exchanges can also be assessed by calculating the theoretical maximum of the magnetic entropy change for isolated Gd^{3+} ions. Indeed, the experimental values for $\mu_0\Delta H$ = 5 T, of 23.3 J kg^{-1} K^{-1} (at 4.5 K) and 54.0 J kg^{-1} K^{-1} (at 2.5 K) for $LiGdS_2$ and $NaGdS_2$ respectively, correspond to 31% and 76% of the theoretical maximum values (*i.e.* 75.7 J kg^{-1} K^{-1} and 70.7 J kg^{-1} K^{-1}, calculated from $Rln(2S+1)/M_w$ with S = 7/2 and M_w($LiGdS_2$) = 228.32 g mol^{-1} and M_w($NaGdS_2$) = 244.37 g mol^{-1}). The magnetocaloric effect is indeed more dramatically hindered by the magnetic interactions occurring in $LiGdS_2$ than in $NaGdS_2$. Hence, the α-$NaFeO_2$ structure type leads to weaker local magnetic interactions and thus to the most significant magnetocaloric properties.

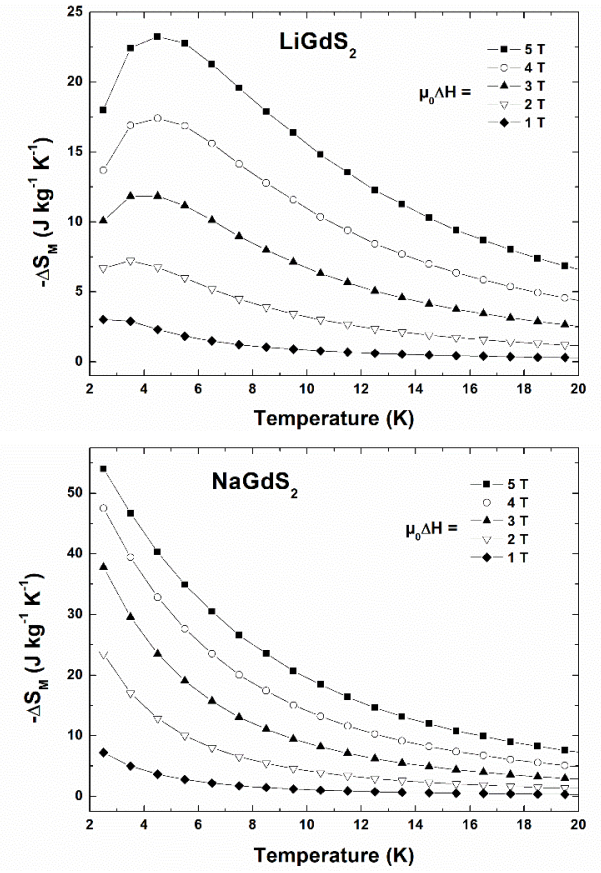

Figure 4. Temperature dependence of the mass magnetic entropy change ($-\Delta S_M$) in (top) $LiGdS_2$ and (bottom) $NaGdS_2$ for different magnetic field variations.

The strength of the magnetic coupling between Gd^{3+} ions can be related to the crystal structure. On the one hand, the NaCl structure type of $LiGdS_2$ corresponds to a semi-ordered three-dimensional structure where Gd atoms are coordinated to six S atoms in regular octahedral environments (6 x $d_{Gd\text{-}S}$ = 2.76 Å). These octahedra interact with each other by sharing edges. By considering that Gd^{3+} and Li^+ are randomly distributed on the same crystallographic site, each Gd atom is surrounded by 12/2 other Gd atoms that are at a mean distance of 3.91 Å. These six Gd neighbours are statistically located in three perpendicular squared planes as illustrated on the left side of Figure 5. Hence, in this semi-ordered structure the Gd···Gd interactions may exist

in the three space directions, favouring local magnetic frustrations and, most likely, leading to spin-glass behaviors. On the other hand, the α-$NaFeO_2$ structure of $NaGdS_2$ consists of two-dimensional $[GdS_2]^-$ layers stacked perpendicularly to the *c* axis and separated by Na^+ cations. Within these layers, each Gd atom is coordinated to six S atoms in a regular octahedral arrangement (6 x $d_{Gd\text{-}S}$ = 2.79 Å) and connected to a neighbouring Gd atom by sharing edges of its octahedron. Hence, each Gd atom is surrounded by six other Gd atoms that are at a distance of 4.01 Å as shown on the right side of Figure 5. These six Gd neighbours form a hexagon and are all located in the *ab* plane, making that in the α-$NaFeO_2$ structure, the Gd···Gd interactions mainly take place in the two-dimensional $[GdS_2]^-$ layers. This perfect triangular 2D Gd lattice should favour magnetic frustrations and, consequently, should suppress or at least significantly lower the antiferromagnetic ordering temperature if any.

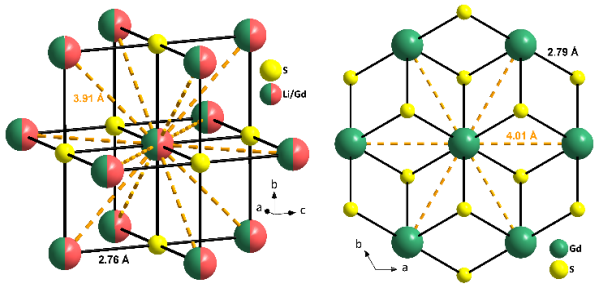

Figure 5. Representation of the gadolinium atoms environments in (left) the NaCl structure type of $LiGdS_2$ and (right) the α-$NaFeO_2$ structure type of $NaGdS_2$. The Gd-S distances are mentioned in black and the Gd···Gd distances in orange. The distances are calculated from refined crystallographic data (Table 1).

From these crystal structure descriptions, one can note that the geometry of the Gd polyhedra are similar in both structures but differ by their connectivities. This results in 3D versus 2D structures for $LiGdS_2$ and $NaGdS_2$ respectively. Moreover, the distances between a Gd atom and its closest Gd neighbours differ from one structure to another, the NaCl structure exhibiting the shortest Gd···Gd interaction distances. Finally, the Li/Gd mixed site occupancy encountered in the NaCl structure type of $LiGdS_2$ probably also affects the magnetic interactions. All of these structural features appear to limit the magnetic decoupling of Gd^{3+} ions in the NaCl structure type and therefore lead to a worsened magnetocaloric effect in $LiGdS_2$. On the contrary, in the α-$NaFeO_2$ structure type, the separation between each $[GdS_2]^-$ layers seems to favor a magnetic decoupling of the Gd^{3+} ions along the *c* axis, and consequently, generates better magnetocaloric properties near liquid helium temperature. Hence, in the $AGdS_2$ series, the reduction of the structure dimensionality together with different Gd environments lead to better magnetocaloric properties for the ordered α-$NaFeO_2$ structure type materials compared to the cationic disordered NaCl structure type one.

Based on the significant magnetocaloric effect observed for $NaGdS_2$, we also decided to assess the magnetocaloric properties of the GdS_2 binary sulfide. This phase can be considered as the "starting point" of the $AGdS_2$ series (i.e. "□GdS_2", the symbol □ corresponding to the alkaline element deficiency) and its large magnetic/non-magnetic mass ratio ($_{wt}$% Gd = 72%) can lead to a promising magnetocaloric effect.

However, attempts to synthesize the nominal GdS_2 phase failed and it appears that high-pressure is mandatory for its synthesis.[76] Following our synthesis protocol, the $Gd_{10}S_{19}$ compound forms preferentially. $Gd_{10}S_{19}$ crystallizes in the $Ce_{10}Se_{19}$ structure type, a three-dimensional tetragonal structure (space group $P4_2/n$) where Gd atoms sit in bicapped and tricapped trigonal prisms that are connected by faces and edges. These structural features clearly differ from those of the $AGdS_2$ members. The magnetic behaviour also deviates from that of the $AGdS_2$ (A = Li, Na, K, Rb) compounds as the existence of an antiferromagnetic ordering at T_N = 5.8 K is detected on the temperature dependant magnetic susceptibility curve (Figure S11). Note that there are structural and physical similarities between $Gd_{10}S_{19}$ and the nominal GdS_2 material; regarding the latter it is reported that (i) Gd coordination polyhedrons are tricapped trigonal prisms sharing faces and edges in a three-dimensional structure and (ii) an antiferromagnetic ordering is observed at T_N = 7.7 K.[76] Using the $Gd_{10}S_{19}$ binary sulfide as a comparison material thus makes sense. The evaluation of its magnetocaloric properties was carried out: the maximum mass magnetic entropy change is reached at 6.5 K with a value of 14.2 J kg^{-1} K^{-1} for $\mu_0\Delta H$ = 5 T which is about four times less than that of $NaGdS_2$ at the same temperature (Figure 4).

The evolution of the maximum mass magnetic entropy change in the $AGdS_2$ (A = Li, Na, K, Rb) family is represented in Figure 6. In addition, as the starting point, $Gd_{10}S_{19}$ is also plotted and denominated as "□GdS_2". This illustrates the benefit of the alkaline element presence and the impact of the structural modification from NaCl to α-$NaFeO_2$. Indeed, the best magnetocaloric effects are obtained for the "layered" α-$NaFeO_2$ structure type materials whatever the alkaline element. Note that the structural modification also influences the temperature for which the effect is maximum.

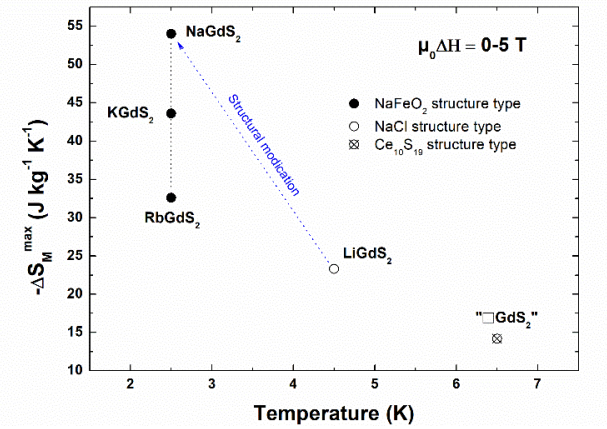

Figure 6. Temperature dependence of the maximum mass magnetic entropy change ($-\Delta S_M^{max}$) for $\mu_0\Delta H$ = 5 T of the $AGdS_2$ (A = Li, Na, K, Rb) family and the "□GdS_2" binary sulfide.

In order to complete our comparison of the $AGdS_2$ series with binary or ternary materials with high magnetic/non-magnetic mass ratio, we also synthesized and characterized three additional compounds: α-Gd_2S_3 sulfide ($_{wt}$% Gd = 77%), Gd_2O_2S ($_{wt}$% Gd = 83%) and Gd_2O_3 ($_{wt}$% Gd = 87%). Their crystallographic data and magnetic measurements are gathered in Table S1 and Figures S12-S14. Tables 3 and S2 summarize structural, magnetic and magnetocaloric properties for both binary and ternary compounds reported in this study. The magnetic behaviours of α-Gd_2S_3 (Figure S14) and Gd_2O_2S (Figure S13) are characterized by long-range antiferromagnetic ordering occurring below T_N = 10.0 K and 6.4 K respectively.

Table 3. Magnetic and magnetocaloric properties of the $AGdS_2$ series (A = Li, Na, K, Rb) compared to those of some Gd-based binary or ternary sulfide/oxysulfide/oxide.

Compound	wt% Gd	T_N (K)	μ_{eff} (μ_B/Gd^{3+})	θ_P (K)	T (K)	$-\Delta S_M^{max}$ (J kg^{-1} K^{-1}) 0-5 T	$-\Delta S_M^{max}$ (mJ cm^{-3} K^{-1}) 0-5 T	ρ_{calc} (g cm^{-3})
"□GdS_2"= $Gd_{10}S_{19}$	72	5.8	7.86(1)	-4.9(1)	6.5	14.2	82.2	5.81
$LiGdS_2$	69	--	7.95(1)	-3.4(1)	4.5	23.3	104.2	4.48
$NaGdS_2$	64	--	7.71(1)	-1.9(1)	2.5	54.0	236.7	4.38
$KGdS_2$	60	--	7.32(1)	-3.7(1)	2.5	43.6	179.5	4.11
$RbGdS_2$	51	--	7.23(1)	-3.3(1)	2.5	32.6	149.9	4.60
α-Gd_2S_3	77	10.0	7.78(1)	-9.9(1)	10.5	0.1	0.9	6.18
Gd_2O_2S	83	6.4	8.12(1)	-21.1(1)	8.5	5.0	36.8	7.33
Gd_2O_3	87	--	7.98(1)	-15.1(1)	4.5	7.9	59.9	7.62

For Gd_2O_3, only local antiferromagnetic couplings are suggested by the negative θ_P value determined from the Curie-Weiss fit (Figure S12). Moreover, despite their high magnetic/non-magnetic mass ratio, none of the binary and ternary additional compounds exhibit better magnetocaloric properties near or below liquid helium temperature than those of the $NaGdS_2$ compound. For most of them, this is mainly related to their antiferromagnetic ordering.

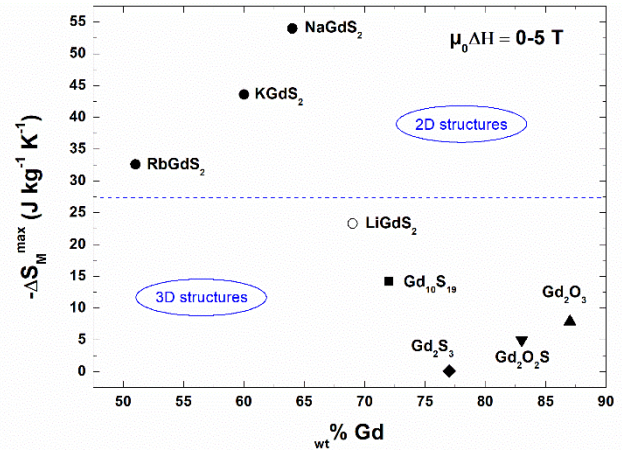

Figure 7. Maximum mass magnetic entropy change ($-\Delta S_M^{max}$) for $\mu_0\Delta H$ = 5 T of $AGdS_2$ (A = Li, Na, K, Rb) members and some binary and ternary Gd-based materials depending on their magnetic/non-magnetic mass ratio ($_{wt}$% Gd). Each symbol corresponds to one structure type.

From a structural point of view, the Gd polyhedra of the binary and ternary sulfide/oxysulfide/oxide are less symmetric compared to those of the $AGdS_2$ members and are all connected within a three-dimensional framework. Regarding the Gd···Gd interaction distances, no obvious correlation with the coordination environment can be made. This is not surprising given that all compounds crystallize in different structure types. Nevertheless, as illustrated in the Figure 7, the structure dimensionality of the studied compounds seems to be an important feature, since the best magnetocaloric properties are observed in the two-dimensional α-$NaFeO_2$ structure type materials. However, on a broader scale, this feature is not the only one that matters. For example, the GdF_3 compound is characterized by a three-dimensional structure and yet is the top ranked inorganic Gd-based magnetic refrigerant near liquid helium temperature.[56] This reflects that magnetocaloric properties depend on several chemical and structural parameters: structure dimensionality, Gd polyhedron symmetry, number of Gd neighbours and their arrangement, Gd···Gd interaction distances, magnetic/non-magnetic mass ratio, etc. All of these influence the nature and the strength of the local magnetic interactions and thus the magnetocaloric effect of Gd-based materials.

Finally, the magnetocaloric properties of some inorganic Gd-based compounds belonging to different material classes (oxides, intermetallics, borides, carbides, borocarbides, inorganic complexes and now sulfides and oxysulfide — details are gathered in Table S3) are illustrated by the Figure 8, where each class is depicted by one symbol. From this figure, one can see that $NaGdS_2$ is well ranked compared to other inorganic Gd-based materials, and especially compared to complexes with light and small ligands represented here by the stars. Moreover, despite their lower wt.% Gd, the $AGdS_2$ (A = K, Rb) sulfides crystallizing in the α-$NaFeO_2$ structure type are also in good position. These results indicate that α-$NaFeO_2$ structural type must be a good starting point for further investigations of magnetic cooling materials.

CONCLUSION

We have synthesized and characterized structurally and magnetically the $AGdS_2$ family (A = Li, Na, K and Rb). Powder X-ray diffraction data evidenced two typical crystal structures within the series: NaCl (for A = Li) and α-$NaFeO_2$ (for A = Na, K, Rb). While the former structure type leads to a moderate magnetocaloric effect near liquid helium temperature, the lower dimensionality of the latter allows to reach the best magnetocaloric properties among the series due to limited magnetic exchange interactions between Gd^{3+} ions. Consequently, $NaGdS_2$ exhibits a magnetocaloric effect comparable to the top ranked inorganic Gd-based materials operating in the cryogenic temperature range, revealing that sulfides can be considered as a new class of promising magnetocaloric materials.

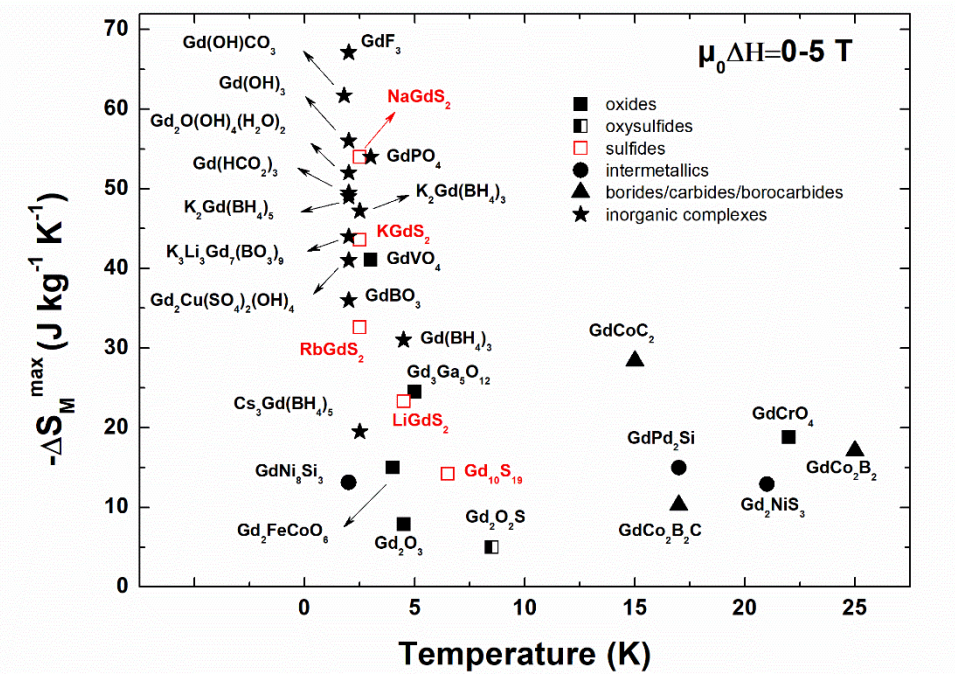

Figure 8. Overview of the maximum mass magnetic entropy change for some Gd-based inorganic materials at cryogenic temperatures ($T \leq 25$ K).[15-16,18-19,21-28,46-56]

AUTHOR INFORMATION

Corresponding author

* (P. Lemoine) E-mail: Pierric.lemoine@univ-rennes1.fr

Author Contributions

The manuscript was written through contributions of all authors. All authors have given approval to the final version of the manuscript.

Note

The authors declare no competing financial interest.

SUPPORTING INFORMATION

Additional figures and tables are available in the supporting information, including PXRD patterns and Rietveld refinements of $AGdS_2$ (A = Li, Na, K, Rb), $Gd_{10}S_{19}$, α-Gd_2S_3 and Gd_2O_2S compounds, crystallographic data of $Gd_{10}S_{19}$, α-Gd_2S_3, Gd_2O_2S, Gd_2O_3 and $AGdS_2$ (A = Li, Na, K, Rb), magnetic and magnetocaloric data of $KGdS_2$ and $RbGdS_2$, magnetic data of $Gd_{10}S_{19}$, Gd_2O_3, Gd_2O_2S and α-Gd_2S_3, and review table on the magnetocaloric properties of inorganic Gd-based materials presented in Figure 8.

ACKNOWLEDGMENTS

Authors are grateful to Thomas Mazet for scientific discussion. The research was supported by the Ministry of Science and Education of the Russian Federation and CNRS through the EMERGENCE@INC 2021 NCIS project.

REFERENCES

(1) Pecharsky, V. K.; Gschneidner, K. A. Magnetocaloric effect and magnetic refrigeration. J. Magn. Magn. Mater. 1999, 200, 44-56.

(2) Tishin, A.; Spichkin, Y. The magnetocaloric effect and its applications, Institute of Physics Publishing, Bristol and Philadelphia, 2003.

(3) Gschneidner, K. A.; Pecharsky, V.; Tsokol, A. Recent developments in magnetocaloric materials. Rep. Progr. Phys. 2005, 68, 1479.

(4) Brück, E. Developments in magnetocaloric refrigeration. J. Phys. D: Appl. Phys. 2005, 38, R381-R391.

(5) Gschneidner, K. A.; Pecharsky, V. Thirty years of near room temperature magnetic cooling: Where we are today and future prospects. Int. J. Refrig. 2008, 31, 945-961.

(6) Numazawa, T.; Kamiya, K.; Utaki, T.; Matsumoto, K. Magnetic refrigerator for hydrogen liquefaction. Cryogenics 2014, 62, 185-192.

(7) Zheng, Y.-Z.; Zhou, G.-J.; Zheng, Z.; Winpenny, R. E. Molecule-based magnetic coolers. Chem. Soc. Rev. 2014, 43, 1462-1475.

(8) Franco, V.; Blázquez, J.; Ipus, J.; Law, J.; Moreno-Ramírez, L.; Conde, A. Magnetocaloric effect: From materials research to refrigeration devices. Prog. Mater. Sci. 2018, 93, 112-232.

(9) Zhang, H.; Gimaev, R.; Kovalev, B.; Kamilov, K.; Zverev V.; Tishin, A. Review on the materials and devices for magnetic refrigeration in the temperature range of nitrogen and hydrogen liquefaction. Physica B Condens. Matter. 2019, 558, 65-73.

(10) Li, L.; Yan, M. Recent progresses in exploring the rare earth based intermetallic compounds for cryogenic magnetic refrigeration. J. Alloys Compd. 2020, 823, 153810.

(11) Giauque, W. A thermodynamic treatment of certain magnetic effects. A proposed method of producing temperatures considerably below, 1(0) absolute. J. Am. Chem. Soc. 1927, 49, 1864-1870.

(12) Giauque, W.; MacDougall, D. Attainment of temperatures below 1 degrees absolute by demagnetization of $Gd_2(SO_4)_3.8H_2O$. Phys. Rev. 1933, 43, 768.

(13) Daudin, B.; Lagnier R.; Salce, B. Thermodynamic properties of the gadolinium gallium garnet, $Gd_3Ga_5O_{12}$, between 0.05 and 25 K. J. Magn. Magn. Mater. 1982, 27, 315-322.

(14) McMichael, R.; Ritter, J.; Shull, R. Enhanced magnetocaloric effect in $Gd_3Ga_{5-x}Fe_xO_{12}$. J. Appl. Phys. 1993, 73, 6946-6948.

(15) Hamilton, A. S.; Lampronti, G.; Rowley, S.; Dutton, S. Enhancement of the magnetocaloric effect driven by changes in the crystal structure of Al-doped GGG, $Gd_3Ga_{5-x}Al_xO_{12}$ ($0 \leq x \leq 5$). J. Phys. Condens. Matter. 2014, 26, 116001.

(16) Dong, Z.; Yin, S. Structural, magnetic and magnetocaloric properties in perovskite RE_2FeCoO_6 (RE = Er and Gd) compounds. Ceram. Int. 2020, 46, 1099-1103.

(17) Midya, A.; Khan, N.; Bhoi D.; Mandal, P. 3d-4f spin interaction and field-induced metamagnetism in $RCrO_4$ (R=Ho, Gd, Lu) compounds. J. Appl. Phys. 2014, 115, 17E114.

(18) Palacios, E.; Tomasi, C.; Sáez-Puche, R.; Dos santos-García, A.; Fernández-Martínez, F.; Burriel, R. Effect of Gd polarization on the large magnetocaloric effect of $GdCrO_4$ in a broad temperature range. Phys. Rev. B 2016, 93, 064420.

(19) Dey, K.; Indra, A.; Majumdar, S.; Giri, S. Cryogenic magnetocaloric effect in zircon-type RVO_4 (R = Gd, Ho, Er, and Yb). J. Mater. Chem. C 2017, 5, 1646-1650.

(20) Rawat R.; Das, I. Magnetocaloric and magnetoresistance studies of $GdPd_2Si$. J. Phys. Condens. Matter. 2001, 13, L57-L63.

(21) Rawat R.; Das, I. Heat capacity and magnetocaloric studies of RPd_2Si (R = Gd, Th and Dy). J. Phys. Condens. Matter. 2006, 18, 1051-1059.

(22) Pakhira, S.; Mazumdar, C.; Ranganathan, R.; Giri S.; Avdeev, M. Large magnetic cooling power involving frustrated antiferromagnetic spin-glass state in R_2NiSi_3 (R = Gd, Er). Phys. Rev. B 2016, 94, 104414.

(23) Pakhira, S.; Mazumdar, C.; Ranganathan, R. Magnetic and magnetocaloric properties of $(Gd_{1-x}Y_x)_2NiSi_3$ compounds (x=0.25, 0.5, 0.75). J. Magn. Magn. Mater. 2019, 484, 456-461.

(24) Pani, M.; Morozkin, A.; Yapaskurt, V.; Provino, A.; Manfrinetti, P.; Nirmala, R.; Malik, S. RNi_8Si_3 (R= Gd,Tb): Novel ternary ordered derivatives of the $BaCd_{11}$ type. J. Solid State Chem. 2016, 233, 397-406.

(25) Li, L.; Nishimura, K.; Yamane, H. Giant reversible magnetocaloric effect in antiferromagnetic $GdCo_2B_2$ compound. Appl. Phys. Lett. 2009, 94, 102509.

(26) Meng, L.; Xu, C.; Yuan, Y.; Qi, Y.; Zhou, S.; Li, L. Magnetic properties and giant reversible magnetocaloric effect in $GdCoC_2$. RSC Adv. 2016, 6, 74765-74768.

(27) Zhang, Y.; Guo, D.; Wu, B.; Wang, H.; Guan, R.; Li, X.; Ren, Z. Magnetic properties and magneto-caloric performances in $RECo_2B_2C$ (RE = Gd, Tb and Dy) compounds. J. Alloys Compd. 2020, 817, 152780.

(28) Li, L.; Kadonaga, M.; Huo, D.; Qian, Z.; Namiki T.; Nishimura, K. Low field giant magnetocaloric effect in RNiBC (R = Er and Gd) and enhanced refrigerant capacity in its composite materials. Appl. Phys. Lett. 2012, 101, 122401.

(29) Zheng, Y. Z.; Evangelisti, M.; Winpenny, R. E. Large Magnetocaloric Effect in a Wells-Dawson Type $\{Ni_6Gd_6P_6\}$ Cage. Angew. Chem. Int. Edit. 2011, 50, 3692-3695.

(30) Peng, J. B.; Zhang, Q. C.; Kong, X. J.; Ren, Y. P.; Long, L. S.; Huang, R. B.; Zheng, L. S.; Zheng, Z. A 48-Metal Cluster Exhibiting a Large Magnetocaloric Effect. Angew. Chem. Int. Edit. 2011, 50, 10649-10652.

(31) Zheng, Y.-Z.; Evangelisti, M.; Winpenny, R. E. Co-Gd phosphonate complexes as magnetic refrigerants. Chem. Sci. 2011, 2, 99-102.

(32) Langley, S. K.; Chilton, N. F.; Moubaraki, B.; Hooper, T.; Brechin, E. K.; Evangelisti, M.; Murray, K. S. Molecular coolers: The case for $[Cu^{II}_5Gd^{III}_4]$. Chem. Sci. 2011, 2, 1166-1169.

(33) Guo, F.-S.; Leng, J.-D.; Liu, J.-L.; Meng, Z.-S.; Tong, M.-L. Polynuclear and Polymeric Gadolinium Acetate Derivatives with Large Magnetocaloric Effect. Inorg. Chem. 2012, 51, 405-413.

(34) Sibille, R. ; Mazet, T.; Malaman, B. ; François, M. A Metal-Organic Framework as Attractive Cryogenic Magnetorefrigerant. Chem. Eur. J 2012, 18, 12970-12973.

(35) Lorusso, G.; Palacios, M. A.; Nichol, G. S.; Brechin, E. K.; Roubeau, O.; Evangelisti, M. Increasing the dimensionality of cryogenic molecular coolers: Gd-based polymers and metal-organic frameworks. Chem. Commun. 2012, 48, 7592-7594.

(36) Guo, F.-S.; Chen, Y.-C.; Liu, J.-L.; Leng, J.-D.; Meng, Z.-S.; Vrábel, P.; Orendáč, M.; Tong, M.-L. A large cryogenic magnetocaloric effect exhibited at low field by a 3D ferromagnetically coupled Mn(II)-Gd(III) framework material. Chem. Commun. 2012, 48, 12219-12221.

(37) Sibille, R.; Didelot, E.; Mazet, T.; Malaman, B.; François, M. Magnetocaloric effect in gadolinium-oxalate framework $Gd_2(C_2O_4)_3(H_2O)_6.(0.6H_2O)$. APL Mater. 2014, 2, 124402.

(38) Li, J.-H.; Liu, A.-J.; Ma, Y.-J.; Han, S.-D.; Hu, J.-X.; Wang, G.-M. A large magnetocaloric effect in two hybrid Gd-complexes: the synergy of inorganic and organic ligands towards excellent cryo-magnetic coolants. J. Mater. Chem. C 2019, 7, 6352-6358.

(39) Pecharsky, V. K.; Gschneidner, K. A. Giant magnetocaloric effect in $Gd_5(Si_2Ge_2)$. Phys. Rev. Lett. 1997, 78, 4494-4497.

(40) Wada, H.; Tanabe, Y. Giant magnetocaloric effect of $MnAs_{1-x}Sb_x$. Appl. Phys. Lett. 2001, 79, 3302-3304.

(41) Tegus, O.; Bruck, E.; Buschow, K. H. J.; de Boer, F. R. Transition-metal-based magnetic refrigerants for room-temperature applications. Nature 2002, 415, 150-152.

(42) Mazet, T.; Ihou-Mouko, H.; Malaman, B. Mn_3Sn_2: A promising material for magnetic refrigeration. Appl. Phys. Lett. 2006, 89, 022503.

(43) Brück, E.; Tegus, O.; Thanh, D.T.C.; Trung, N.T.; Buschow, K.H.J. A review on Mn based materials for magnetic refrigeration: Structure and properties. International Journal of Refrigeration 2008, 31, 763-770.

(44) Manoli, M.; Johnstone, R. D. L.; Parsons, S.; Murrie, M.; Affronte, M.; Evangelisti, M.; Brechin, E. K. A ferromagnetic mixed-valent Mn supertetrahedron: Towards low-temperature magnetic refrigeration with molecular clusters. Angew. Chem. Int. Ed. 2007, 46, 4456-4460.

(45) Evangelisti, M.; Roubeau, O.; Palacios, E.; Camon, A.; Hooper, T. N.; Brechin, E. K.; Alonso, J. J. Cryogenic Magnetocaloric Effect in a Ferromagnetic Molecular Dimer. Angew. Chem. Int. Ed. 2011, 50, 6606-6609.

(46) Palacios, E.; Rodríguez-Velamazán, J.; Evangelisti, M.; McIntyre, G.; Lorusso, G.; Visser, D.; de Jongh L. J.; Boatner, L. A. Magnetic structure and magnetocalorics of $GdPO_4$. Phys. Rev. B 2014, 90, 214423.

(47) Xia, M.; Shen, S.; Lu, J.; Sun, Y.; Li, R. $K_3Li_3Gd_7(BO_3)_9$: A New Gadolinium-Rich Orthoborate for Cryogenic Magnetic Cooling. Chem. Eur. J 2018, 24, 3147-3150.

(48) Mukherjee, P.; Wu, Y.; Lampronti, G.; Dutton, S. Magnetic properties of monoclinic lanthanide orthoborates, $LnBO_3$, Ln = Gd, Tb, Dy, Ho, Er, Yb. Mater. Res. Bull 2018, 98, 173-179.

(49) Tang, Y.; Guo, W.; Zhang, S.; Yang, M.; Xiang, H.; He, Z. $Gd_2Cu(SO_4)_2(OH)_4$: a 3d-4f hydroxysulfate with anenhanced cryogenic magnetocaloric effect. Dalton Trans. 2015, 44, 17026-17029.

(50) Han, Y.; Han, S.-D.; Pan, J.; Ma, Y.-J.; Wang, G.-M. An excellent cryogenic magnetic cooler: magnetic and magnetocaloric study of an inorganic frame material. Mater. Chem. Front. 2018, 2, 2327-2332.

(51) Chen, Y.-C.; Qin, L.; Meng, Z.-S.; Yang, D.-F.; Wu, C.; Fu, Z.; Zheng, Y.-Z.; Liu, J.-L.; Tarasenko, R.; Orendáč, M. Study of a magnetic-cooling material $Gd(OH)CO_3$. J. Mater. Chem. A 2014, 2, 9851-9858.

(52) Lorusso, G.; Sharples, J. W.; Palacios, E.; Roubeau, O.; Brechin, E. K.; Sessoli, R.; Rossin, A.; Tuna, F.; McInnes, E. J.; Collison, D. A Dense Metal-Organic Framework for Enhanced Magnetic Refrigeration. Adv. Mater 2013, 25, 4653-4656.

(53) Saines, P. J.; Paddison, J. A.; Thygesen P. M.; Tucker, M. G. Searching beyond Gd for magnetocaloric frameworks: magnetic properties and interactions of the $Ln(HCO_2)_3$ series. Mater. Horiz. 2015, 2, 528-535.

(54) Schouwink, P.; Didelot, E.; Lee, Y.-S.; Mazet, T.; Černý, R. Structural and magnetocaloric properties of novel gadolinium borohydrides. J. Alloys Compd. 2016, 664, 378-384.

(55) Yang, Y.; Zhang, Q.-C.; Pan, Y.-Y.; Long, L.-S.; Zheng, L.-S. Magnetocaloric effect and thermal conductivity of $Gd(OH)_3$ and $Gd_2O(OH)_4(H_2O)_2$. Chem. Commun. 2015, 51, 7317-7320.

(56) Chen, Y.-C.; Prokleška, J.; Xu, W.-J.; Liu, J.-L.; Liu, J.; Zhang, W.-X.; Jia, J.-H.; Sechovský, V.; Tong, M.-L. A brilliant cryogenic magnetic coolant: magnetic and magnetocaloric study of ferromagnetically coupled GdF_3. J. Mater. Chem. C 2015, 3, 12206-12211.

(57) Li, D.; Yamamura, T.; Nimori, S.; Homma, Y.; Honda, F.; Haga, Y.; Aoki, D. Large reversible magnetocaloric effect in ferromagnetic semiconductor EuS. Solid State Commun. 2014, 193, 6-10.

(58) Li, L.; Hirai, S.; Nakamura, E.; Yuan, H. Influences of Eu_2O_3 characters and sulfurization conditions on the preparation of EuS and its large magnetocaloric effect. J. Alloys Compd. 2016, 687, 413-420.

(59) Zheng, X.-C.; Li, X.-Y.; He, L.-H.; Zhang, S.-Y.; Tang, M.-H.; Wang, F.-W. Magnetic properties and magnetocaloric effect of the Cr-based spinel sulfides $Co_{1-x}Cu_xCr_2S_4$. Chinese Phys. B 2017, 26, 037502.

(60) Bouhbou, M.; Moubah, R.; Belayachi, W.; Belayachi, A.; Bessais L.; Lassri, H. Magnetic and magnetocaloric properties in sulfospinel $Cd_{1-x}Zn_xCr_2S_4$ (x=0, 0.3, 0.5) powders. Chem. Phys. Lett. 2017, 688, 84-88.

(61) Fukuda, H.; Kobayashi, Y.; Arai, R.; Baba, K.; Nakagome H.; Numazawa, T. Magneto Caloric Properties of Polycrystalline Gd_2O_2S for an Adiabatic Demagnetization Refrigerator, MATEC Web of Conferences 2017, 109, 04004.

(62) Guo, Q.; Tegus O.; Ebisu, S. Specific heat in magnetic field and magnetocaloric effects of alpha-R_2S_3 (R = Tb, Dy) single crystals. J. Magn. Magn. Mater. 2018, 465, 260-269.

(63) Dey, K.; Indra, A.; Karmakar, A.; Giri, S. Multicaloric effect in multiferroic sulpho spinel MCr_2S_4 (M = Fe & Co). J. Magn. Magn. Mater. 2020, 498, 166090.

(64) Ballestracci, R. Etude cristallographique de nouveaux sulfures de terres rares et de metaux alcalins M = Li, K. Bull. Soc. Franc. Miner. Crist. 1965, LXXXVIII, 207-210.

(65) Sato, M.; Adachi G.; Shiokawa, J. Preparation and structure of sodium rare-earth sulfides, $NaLnS_2$ (Ln; rare earth elements). Mat. Res. Bull. 1984, 19, 1215-1220.

(66) Ohtani, T.; Honjo H.; Wada, H. Synthesis, order-disorder transition and magnetic properties of $LiLnS_2$, $LiLnSe_2$, $NaLnS_2$ and $NaLnSe_2$ (Ln=Lanthanides). Mat. Res. Bull. 1987, 22, 829-840.

(67) Cotter, J. P.; Fitzmaurice, J. C.; Parkin, I. P. New routes to alkali-metal-rare-earth-metal sulfides. J. Mater. Chem. 1994, 4, 1603-1610.

(68) Fabry, J.; Havlak, L.; Dusek, M.; Vanek, P.; Drahokoupil, J.; Jurek, K. Structure determination of $KLaS_2$, $KPrS_2$, $KEuS_2$, $KGdS_2$, $KLuS_2$, KYS_2, $RbYS_2$, $NaLaS_2$ and crystal-chemical analysis of the group 1 and thallium(I) rare-earth sulfide series. Acta Cryst. 2014, B70, 360-371.

(69) Fabry, J.; Havlak, L.; Kucerakova M.; Dusek, M. Redetermination of $NaGdS_2$, $NaLuS_2$ and $NaYS_2$. Acta Cryst. 2014, C70, 533-535.

(70) Luo, X.; Ma, L.; Xing, M.; Fu, Y. ; Zhou, X.; Sun, M. Preparation of $NaGdS_2$ via thermolysis of $Gd[S_2CN(C_4H_8)]_3$-phen complexes and sodium diethyldithiocarbamate mixtures. Mat. Res. Bull. 2013, 48, 1999-2001.

(71) Ohta, M.; Hirai, S.; Kato, H.; Sokolov V.V.; Bakovets, V.V. Thermal Decomposition of NH_4SCN for Preparation of Ln_2S_3 (Ln = La and Gd) by Sulfurization. Mater.Trans. 2009, 50, 1885-1889.

(72) Pomelova, T. A.; Podlipskaya, T. Y.; Kuratieva, N. V.; Cherkov, A. G.; Nebogatikova, N. A.; Ryzhikov, M. R.; Huguenot, A.; Gautier, R.; Naumov, N. G. Synthesis, crystal structure, and liquid exfoliation of layered lanthanide sulfides KLn_2CuS_6 (Ln = La, Ce, Pr, Nd, Sm). Inorg. Chem. 2018, 57, 13594-13605.

(73) Rodriguez-Carvajal, J. Recent advances in magnetic structure determination by neutron powder diffraction. Phys. B 1993, 192, 55-69.

(74) Roisnel, T.; Rodriguez-Carvajal, J. WinPLOTR: A Windows tool for powder diffraction pattern analysis. Mater. Sci. Forum 2001, 378-381, 118-123.

(75) Pecharsky, V.; Gschneidner, K.A. Magnetocaloric effect from indirect measurements: Magnetization and heat capacity. J. Appl. Phys. 1999, 86, 565-575.

(76) Müller, C. J.; Schwarz, U.; Schmidt, P.; Schnelle, W.; Doert, T. High-Pressure Synthesis, Crystal Structure, and Properties of GdS_2 with Thermodynamic Investigations in the Phase Diagram Gd-S. Z. Anorg. Allg. Chem 2010, 636, 947-953